Supporting Information

Böhm et al. 10.1073/pnas.1217745110

SI Materials and Methods

Construction of Cysteine Variants. Cysteine residues replacing MalG-T46, MalE-T36, MalE-S352, and MalK-V17/E128 were introduced by site-directed mutagenesis into the respective plasmid-borne alleles using the Stratagene's Quik change mutagenesis kit according to the manufacturer's instructions. Constructions of MalG-P78C, MalE-G13C, MalE-S211C, and MalE-T80C were described elsewhere (1, 2).

Purification of $MalFGK_2$ and MalE Variants and Spin Labeling. Histidine-tagged $MalFGK_2$ variants were overproduced and purified essentially as described earlier (3), except for omitting $MgCl_2$ from all buffers. Briefly, cells were disrupted by one passage through a French Press at 18,000 psi. The membrane fraction was isolated by centrifugation (200,000 × *g* for 1 h at 4 °C) and resuspended at a total protein concentration of 5 mg/mL in 50 mM Tris·HCl (pH 7.5), 20% (vol/vol) glycerol, and 1.1% (wt/vol) n-dodecyl-β-D-maltoside (buffer 1). After incubation for 1 h on ice, extracted proteins were separated from the remaining membrane fraction by ultracentrifugation and subsequently subjected to Nickel-Nitrilotriacetic acid (Ni-NTA) chromatography. Pooled complex protein-containing fractions were desalted by passage through a PD10 desalting column (GE Healthcare), equilibrated with 50 mM Tris (pH 7.5), 10% (vol/vol) glycerol, and 0.2% n-dodecylß-D-maltoside (buffer 2). His_6–MalE (wild type and variants) was purified from the cytosolic fraction of *Escherichia coli* strain JM109 harboring plasmid pCB06 or derivatives according to (2). To remove tightly bound maltose, purified MalE variants were subjected to a denaturation/renaturation procedure using 6 M guanidine hydrochloride as described in ref. 4. Cysteine mutants of MalE (20 μM protein concentration) were spin-labeled with a 10-fold molar excess of MTSSL [(1-Oxyl-2,2,5,5-tetramethylpyrrolidin-3-yl) methyl methanethiosulfonate label Toronto Research Chemicals] and incubated 1 h at 4 °C under gentle shaking. Excess of MTSSL was removed with a PD10 column and the labeled protein was concentrated to approximately 200 μM. Spin-labeling efficiency was about 80–90%. The cysteine mutants of the transporter were spin labeled with the same procedure but using a 2–4-fold molar excess of MTSSL with respect to the cysteines.

Labeling with 2-(4′-Maleimidylanilino)Naphthalene-6-Sulfonic Acid. MIANS [2-(4′-maleimidylanilino)naphthalene-6-sulfonic acid] modification of $MalFGK(V17C/E128C)_2$ was performed after cross-linking of 2.5 μM of complex in the presence of 5 μM wild-type MalE, 4 mM ATP, and 1 μM 1,6 hexandiyl-bismethanethiosulfonate (HBS) as described in ref. 5, except that buffer 2 was used and no dithiothreitol (DTT) was added to terminate the reaction.

Preparation of Proteoliposomes. For ATPase activity measurements, $MalFGK_2$ variants were reconstituted into liposomes at a lipid to protein ratio of 50:1 (*E. coli* total lipid extract; Avanti Polar Lipids). Reconstitution was performed by incubating the mixture with Bio-Beads (100 mg; Bio-Rad) for 18 h at 4 °C. Proteoliposomes were isolated by centrifugation at 200,000 × *g* for 1 h at 4 °C, and the equivalent of 100 μg complex (determined by quantitation of MalK after SDS/PAGE) was resuspended in 600 μL buffer 3 containing 50 mM Tris·HCl (pH 7.5). For site-specific cross-linking, $MalFGK_2$ variants were reconstituted at a 10:1 lipid-to-protein ratio in the absence or presence of 10 mM ADP or 10 mM ATP. $MalFGK(V17C/E128C)_2$ was reconstituted in the presence of a twofold molar excess of wild-type MalE. After incubation with Bio-Beads (300 mg) for 1 h at 4 °C the equivalent of 100 μg of complex was resuspended in 120 μL of buffer 3.

For double electron–electron resonance (DEER) measurements, transporters were reconstituted at a 10:1 lipid-to-protein ratio either in the absence of nucleotides or in the presence of 5 mM AMP–PNP (adenylylimidodiphosphate). The total assay comprised 1 mL total volume, 700 μg transporter, and 800 μg MalE. For suitable sample concentrations, after centrifugation at 180,000 × *g* the whole amount was resuspended in buffer 3. We stepwise added 10 mM $MgCl_2$ to the reconstituted samples before DEER measurements.

Cross-Linking Experiments. Cross-linking experiments using homobifunctional thiosulfonate linkers were performed as described earlier (5). In brief, the thiosulfonate cross-linkers 1,2 ethanediyl-bismethanethiosulfonate (EBS), HBS, and 3,6,9,12,15-pentaoxaheptadecan-1,17-diyl-bis-methanethiosulfonate (PBS) with approximate spacer lengths of 5.2 Å, 10.4 Å, and 24.7 Å, respectively (6), were purchased from Toronto Chemicals. After incubation of the indicated protein samples (2.5 μM $MalFGK_2$ variants, 5 μM MalE variants) in buffer 2 for 10 min at 37 °C, reactions were started by adding the respective cross-linker (final concentration 1 mM). After 20 min at room temperature, reactions were terminated by adding 5 mM *N*-ethylmaleimide. Additives used were ADP (4 mM), ATP (4 mM), maltose (10 μM), $MgCl_2$ (10 mM), and vanadate (0.5 mM).

For ATPase measurements of cross-linked MalE–FGK_2 complexes, cross-linking reactions were carried with the respective protein samples in the presence of 10 μM maltose and 5 mM of PBS or EBS as indicated for 20 min at room temperature. Subsequently, cross-linked complexes were isolated by size-exclusion chromatography (Superdex 200, GE Healthcare) in buffer 2.

Cross-linking of complex variants reconstituted in the absence or presence of ADP or ATP were performed essentially as described above, with the exception of using 5 μM $MalFGK_2$ variants and 10 μM MalE variants, unliganded or supplemented with 20 μM maltose, in 50 mM Tris (pH 7.5). Vanadate-trapped complexes were prepared as described in ref. 5.

ATPase Assay. ATPase measurements were carried out with reconstituted complex variants at a final protein concentration of 0.5 μM in 50 mM Tris (pH 7.5), 5 mM $MgCl_2$ buffer. The respective purified MalE variant was added at a constant concentration of 5 μM in the absence or presence of 20 μM maltose. The reaction was initiated by addition of 2 mM ATP and ATP hydrolysis was measured by assaying the release of inorganic phosphate at 37 °C using ammonium molybdate as described in ref. 7.

Activity measurements of $MalFGK_2$ variants and cross-linked complexes in detergent solution were performed accordingly except for using 10 mM $MgCl_2$. Purified MalE variants were added to a final concentration of 5 μM. Incorporated into proteoliposomes, all complex variants displayed basal ATPase activities that were slightly increased by open unliganded MalE and further stimulated in the presence of maltose-loaded MalE. In detergent solution, stimulation of the intrinsic enzymatic activity by MalE was also observed but less pronounced, consistent with earlier reports (8–10) (Tables S1 and S2). All MalG and MalK cys mutations were found to be active before and after spin labeling (Tables S1 and S2). Spin-labeled MalE variants stimulated the activity of the wild-type complex between 67% and 102% compared with the unlabeled protein, with the exception of MalE (G13R1), which was not further considered for EPR experiments (Table S1).

Transport Assay of [^{14}C] Maltose. Transport of [^{14}C] maltose was measured using proteoliposomes formed by fast dilution of 100 μg of the indicated complex variants mixed with 250 μL of *E. coli* total lipids sonicated in 50 mM Tris·HCl (pH 7.5), 25 μL 10% (wt/vol) octyl β-D-glucopyranoside in 30 mL 50 mM Tris·HCl (pH 7.5) containing 7.5 mM ATP. After ultracentrifugation at 200,000 × g for 30 min, proteoliposomes were resuspended in 400 μL 50 mM Tris·HCl (pH 7.5). For transport assays, 60 μL of proteoliposomes (final complex concentration of 0.5 μM) were mixed with MalE(G13C) or MalE(S352C) variants (final concentrations of 5 μM and 0.5 μM, respectively) and 10 μM [^{14}C] maltose (600 μCi/μmol; American Radiolabeled Chemicals) in 50 mM Tris·HCl (pH 7.5) buffer containing 1 mM $MgCl_2$. After 20, 40, 60, and 80 s, 25 μL aliquots were diluted in 1 mL 50 mM Tris·HCl (pH 7.5) containing 1 mM maltose followed by rapid filtration through a 0.22 μm nitrocellulose Millipore filter. Subsequently, the filters were washed once with 5 mL of 50 mM Tris·HCl (pH 7.5), and retained radioactivity was determined by liquid scintillation counting. For the cross-linked supercomplexes, no MalE was added. For background correction, proteoliposomes without ATP were used.

DEER Experiments and Simulations. DEER traces were recorded on detergent-solubilized transporters in three different conditions: absence of nucleotides (apo-state), 3 mM ATP to 0.075 mM EDTA (ATP-state), and 3 mM ADP to 5 mM $MgCl_2$ (ADP-state). The proteoliposome samples contained AMP–PNP instead of ATP/EDTA.

DEER measurements were performed at Q-band frequencies (34–35 GHz) on a homemade spectrometer equipped with a traveling-wave-tube amplifier (150 W) and a home-made rectangular resonator enabling the insertion of sample tubes with 3 mm outer diameter (11). Dipolar time evolution data were acquired using the four-pulse DEER experiment. All DEER measurements were performed at 50 K. All pulses were set to 12 ns, and deuterium nuclear modulations were averaged by increasing the first interpulse delay by 16 ns for eight steps. The electron double resonance frequency was set at the maximum of the echo-detected field swept spectrum, 80 MHz higher than the observed frequency. The background of the DEER primary data [V(t)] was fitted and the resulting secondary data [F(t)] were converted by a model-free Tikhonov regularization to distance distributions with the software DeerAnalysis2011 (12). Few DEER measurements were also performed at X band with the conventional scheme. The observer frequency was 65 MHz higher than the pump frequency, and all observer pulses were set to 32 ns and the pump pulse to 12 ns. Hydrogen and deuterium modulation artifacts were averaged (eight times increment of 56 ns). All samples were prepared independently from different batches, and the DEER traces were found to be reproducible. Samples for DEER measurements contained 10% (vol/vol) d8-glycerol and were shock-frozen in liquid nitrogen before being inserted in the precooled cavity at 50 K.

The simulation of the possible spin-label rotamers attached at positions in $MalFGK_2$-E was performed using the Matlab program package MMM based on a rotamer library approach (13).

The low affinity of MalE to $MalFGK_2$ results in low modulation depths of the DEER traces, which dramatically decreases the S–N ratio. With the usual concentrations for DEER (~150 μM transporter and ~300 μM MalE), the maximal modulation depth assuming a K_d of about 10^{-4} M and 100% labeling efficiency is estimated to be 0.2. Measuring in Q band is advantageous to maximize the S–N ratio and to avoid residual artifacts due to modulation of the signal with proton and deuterium frequencies.

It is worth noting that $MalK_2$ is a symmetric homodimer; thus, spin-labeling of the double cysteine mutants (V17C–E128C) in the nucleotide-binding domains (NBDs) leads to a four-spin system with inherent peculiarities. The 17–128′ (the prime denotes the second MalK monomer) and the 128–17′ pairs are characterized by short distances, which should report the closure and reopening of the NBDs and are clearly separable from the longer distances between the other intra- and inter-MalK pairs. Moreover, due to the separation between the different dipolar frequencies, ghost peaks (14) resulting from four spin artifacts were found to be negligible.

1. Daus ML, Grote M, Schneider E (2009) The MalF P2 loop of the ATP-binding cassette transporter MalFGK2 from Escherichia coli and Salmonella enterica serovar typhimurium interacts with maltose binding protein (MalE) throughout the catalytic cycle. *J Bacteriol* 191(3):754–761.
2. Daus ML, Berendt S, Wuttge S, Schneider E (2007) Maltose binding protein (MalE) interacts with periplasmic loops P2 and P1 respectively of the MalFG subunits of the maltose ATP binding cassette transporter (MalFGK(2)) from Escherichia coli/Salmonella during the transport cycle. *Mol Microbiol* 66(5):1107–1122.
3. Landmesser H, et al. (2002) Large-scale purification, dissociation and functional reassembly of the maltose ATP-binding cassette transporter ($MalFGK_2$) of *Salmonella typhimurium*. *Biochim Biophys Acta* 1565(1):64–72.
4. Hall JA, Davidson AL, Nikaido H (1998) Preparation and reconstitution of membrane-associated maltose transporter complex of *Escherichia coli*. *Methods Enzymol* 292: 20–29.
5. Daus ML, et al. (2007) ATP-driven MalK dimer closure and reopening and conformational changes of the "EAA" motifs are crucial for function of the maltose ATP-binding cassette transporter ($MalFGK_2$). *J Biol Chem* 282(31):22387–22396.
6. Loo TW, Clarke DM (2001) Determining the dimensions of the drug-binding domain of human P-glycoprotein using thiol cross-linking compounds as molecular rulers. *J Biol Chem* 276(40):36877–36880.
7. Nikaido K, Liu PQ, Ames GF (1997) Purification and characterization of HisP, the ATP-binding subunit of a traffic ATPase (ABC transporter), the histidine permease of *Salmonella typhimurium*. Solubility, dimerization, and ATPase activity. *J Biol Chem* 272(44):27745–27752.
8. Chen J, Sharma S, Quiocho FA, Davidson AL (2001) Trapping the transition state of an ATP-binding cassette transporter: Evidence for a concerted mechanism of maltose transport. *Proc Natl Acad Sci USA* 98(4):1525–1530.
9. Reich-Slotky R, Panagiotidis C, Reyes M, Shuman HA (2000) The detergent-soluble maltose transporter is activated by maltose binding protein and verapamil. *J Bacteriol* 182(4):993–1000.
10. Daus ML, et al. (2007) ATP-driven MalK dimer closure and reopening and conformational changes of the "EAA" motifs are crucial for function of the maltose ATP-binding cassette transporter ($MalFGK_2$). *J Biol Chem* 282(31):22387–22396.
11. Polyhach Y, et al. (2012) High sensitivity and versatility of the DEER experiment on nitroxide radical pairs at Q-band frequencies. *Phys Chem Chem Phys* 14(30): 10762–10773.
12. Jeschke G, et al. (2006) DeerAnalysis2006—A comprehensive software package for analyzing pulsed ELDOR data. *Appl Magn Reson* 30(3-4):473–498.
13. Polyhach Y, Bordignon E, Jeschke G (2011) Rotamer libraries of spin labelled cysteines for protein studies. *Phys Chem Chem Phys* 13(6):2356–2366.
14. Jeschke G, Sajid M, Schulte M, Godt A (2009) Three-spin correlations in double electron-electron resonance. *Phys Chem Chem Phys* 11(31):6580–6591.

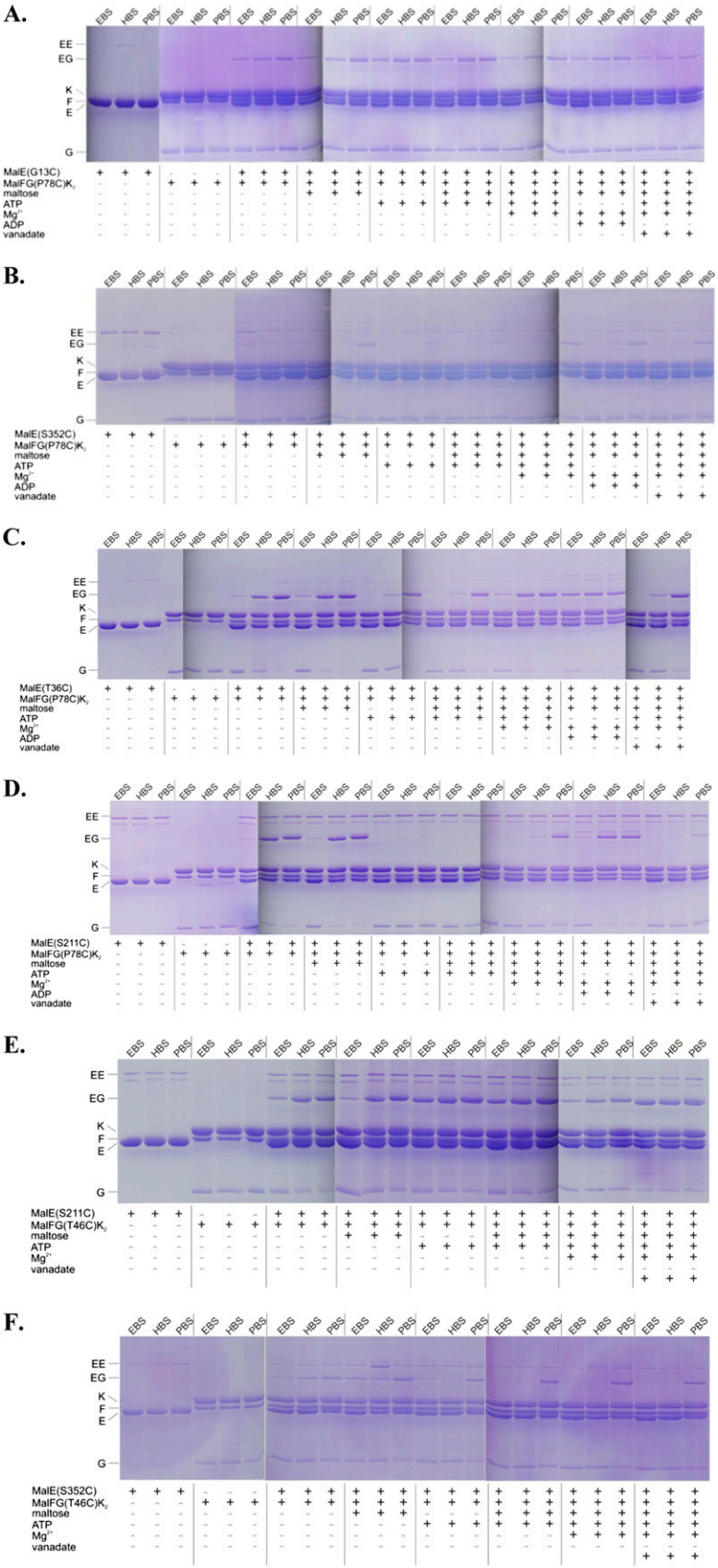

Fig. S1. Site-specific cross-linking of MalFGK$_2$ to *N*- and C-lobe cysteine variants of MalE. Homobifunctional thiosulfonate cross-linkers with defined spacer lengths (EBS, 5.2 Å; HBS, 10.4 Å; PBS, 24.7 Å) and cofactors were added to different combinations of MalE-transporter cysteine mutants as described in the figure either in liposomes (*A* and *B*) or in detergent (*C*–*F*). The results of the SDS/PAGE are presented.

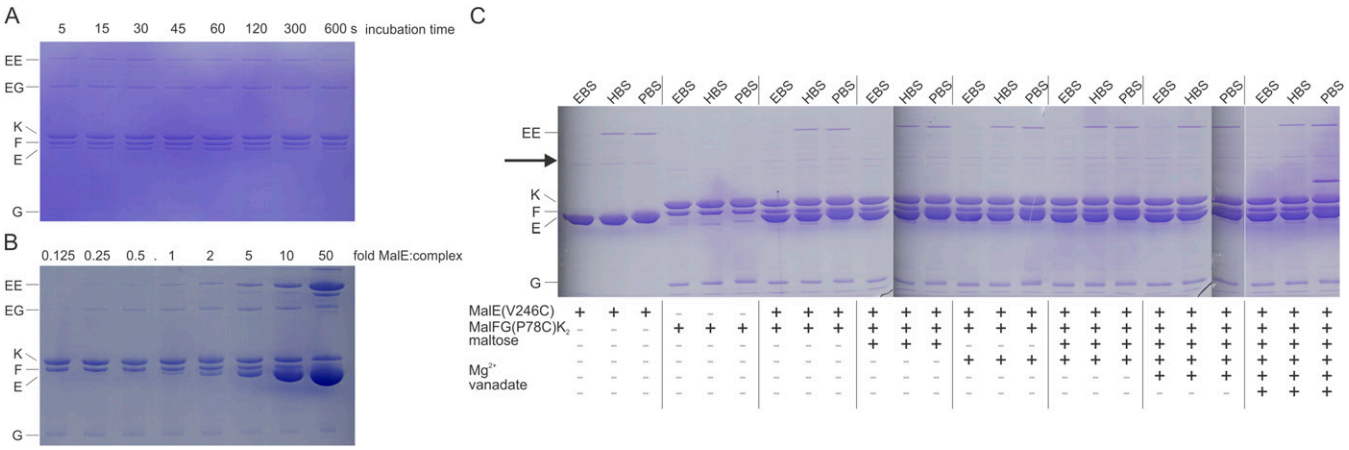

Fig. S2. SDS/PAGE analyses of cross-linked products obtained under varying experimental conditions in n-Dodecyl β-D-maltoside micelles. (*A*) Time-dependent cross-linking of MalFG(T46C)K_2 (2.5 μM) with MalE(S211C) (5 μM) in the presence of maltose (10 μM) and low concentration of the homobifunctional thiosulfonate cross-linker HBS (1 μM). (*B*) MalFG(T46C)K_2 (2.5 μM) was incubated for 5 s with n-fold molar excess of MalE(S211C) in the presence of maltose (10 μM) and HBS (1 μM). (*C*) MalFG(P78)K_2 (2.5 μM) was incubated with MalE(V246C) (5 μM) and linkers with defined spacer lengths (EBS, 5.2 Å; HBS, 10.4 Å; PBS, 24.7 Å, 1 mM) in the presence of cofactors as indicated. The arrow marks the position where the MalE-MalG cross-linked band (EG band) would appear. No cross-linked EG band is visible under the conditions tested. Please note that the faint band always present around this molecular weight is a contaminant of the MalE (V246C) preparation (first three lanes).

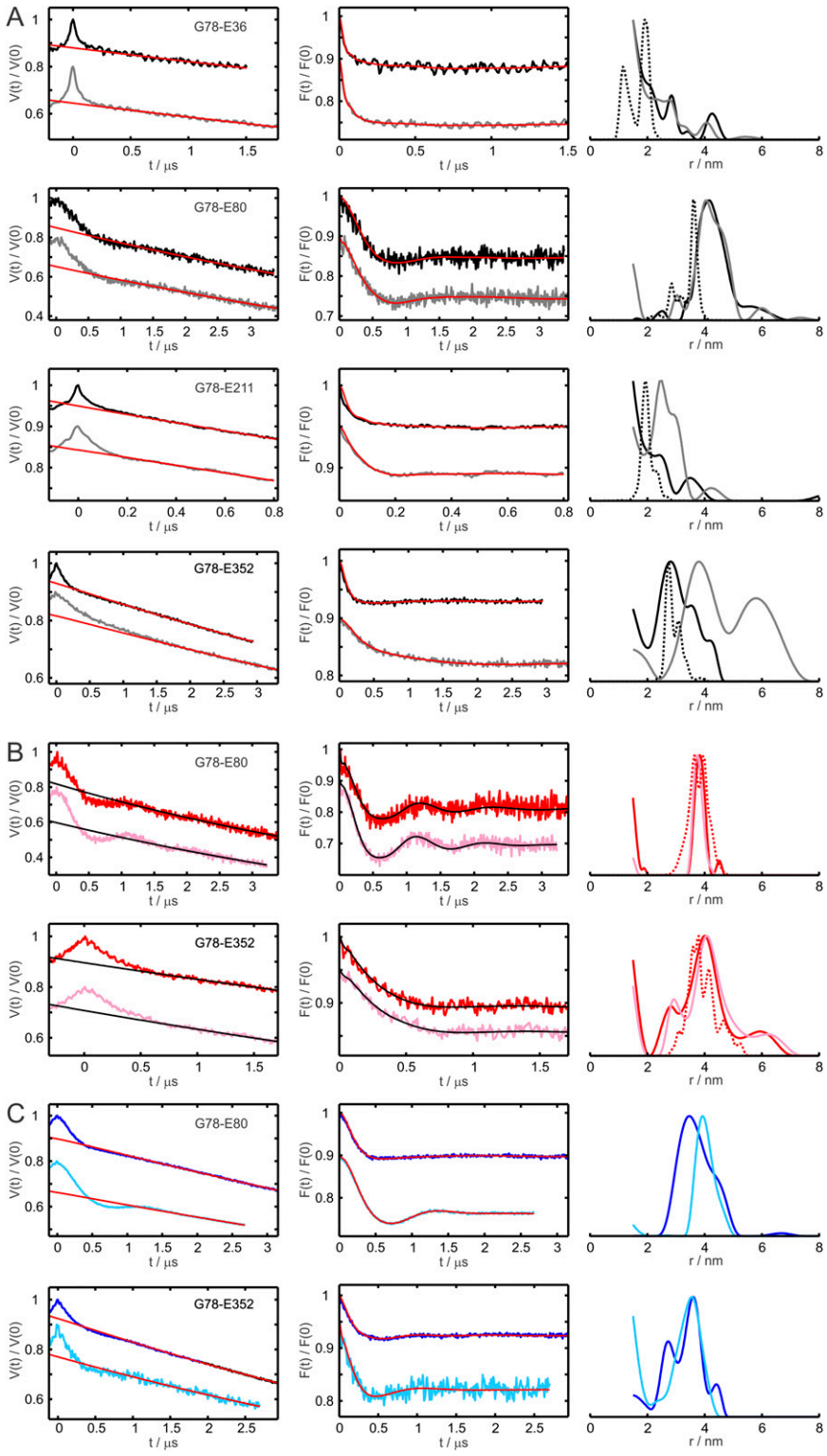

Fig. S3. Experimental interspin distances between MalE and MalG compared with simulations. (*Left*) DEER primary data V(t) and background fits obtained with DeerAnalysis2011. (*Middle*) Normalized DEER form factors F(t) and corresponding fits. (*Right*) Distance distributions obtained with Tikhonov regularization parameters 100 or 1,000. For clarity, the mutants are named according to the subunit at which the spin label is attached and the amino acid position (e.g., G78, E36). (*A*) Apo-state, in the presence (black) and absence (gray) of maltose. (*B*) ATP–EDTA-state, in the presence (red) and absence (pink) of maltose. (*C*) ADP–state, in the presence (blue) and absence (cyan) of maltose. The dotted lines show the corresponding simulated distance distribution performed with MMM based on the crystal structure of the apo-state [Protein Data Bank (PDB) 3PV0, black] and of the AMP–PNP-state (PDB 3PUY, red).

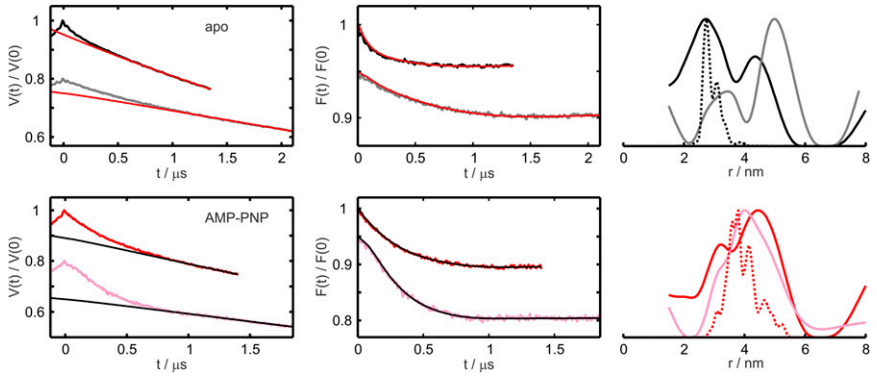

Fig. S4. Maltose effect on reconstituted samples. DEER analysis of the mutant pair MalFG(P78R1)K_2–MalE(S352R1) reconstituted into liposomes. (*Upper*) Apo state in presence (black) and absence (gray) of 10 mM maltose. (*Lower*) AMP–PNP (10 mM) was added during reconstitution in the presence (red) and absence (pink) of 10 mM maltose. (*Left*) Normalized DEER raw data V(t) and background fits obtained with DeerAnalysis2011. (*Middle*) Normalized DEER form factors F(t) and fits obtained with DeerAnalysis2011. (*Right*) Distance distributions obtained with Tikhonov regularization parameter 1,000. The results of the corresponding simulated distance distribution (dotted black, dotted red) performed with MMM based on the crystal structures of the apo- (3PV0) and AMP–PNP- (3PUY) state are superimposed to the experimental distance distributions.

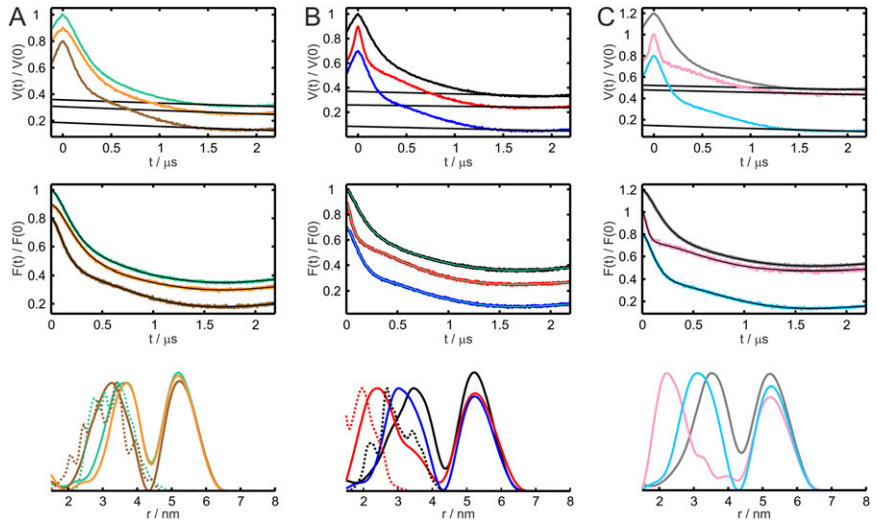

Fig. S5. MalE and maltose effects on $MalK_2$ interspin distances in different nucleotide states (different comparisons with respect to Fig. 4). (*Upper*) Normalized DEER primary data V(t) and background fits obtained with DeerAnalysis2011 on $MalFGK_2$ transporters solubilized in DDM spin labeled at positions 17 and 128 in MalK. (*Middle*) Normalized DEER form factors F(t) and fits obtained with DeerAnalysis2011. (*Bottom*) Corresponding distance distributions obtained with Tikhonov regularization. The short distance peak (< 4.5 nm) represents the 17–128′ and 128–17′ contributions. (*A*) $MalFGK_2$ transporter alone in the apo-state (turquoise), AMP–PNP–Mg^{2+} (10 mM, orange trace), and ADP–Mg^{2+} (10 mM, brown trace). (*B*) Analogous DEER analysis performed after incubation of $MalFGK_2$ with WT–MalE and 1 mM maltose without nucleotides (black), in the presence of AMP–PNP–Mg^{2+} (10 mM, red trace) or ADP–Mg^{2+} (10 mM, blue trace). (*C*) Analogous DEER analysis performed after incubation with WT–MalE in the absence of maltose without nucleotides (gray), with AMP–PNP–Mg^{2+} (pink) and ADP–Mg^{2+} (cyan). The distance distributions obtained from simulations with MMM are superimposed as dotted lines in the color of the corresponding state. For clarity only the 128–17′ and 17–128′ distance contributions are shown. The interspin distances of the transporter alone (*A*) are based on PDB 3FH6 (turquoise) and PDB 2AWO (brown), the latter representing only the isolated NBDs in the ADP-state. In case of $MalFGK_2$-E-complexes in the presence of maltose (*B*), the simulations are based on PDB 3PV0 (black) and 3PUY (red).

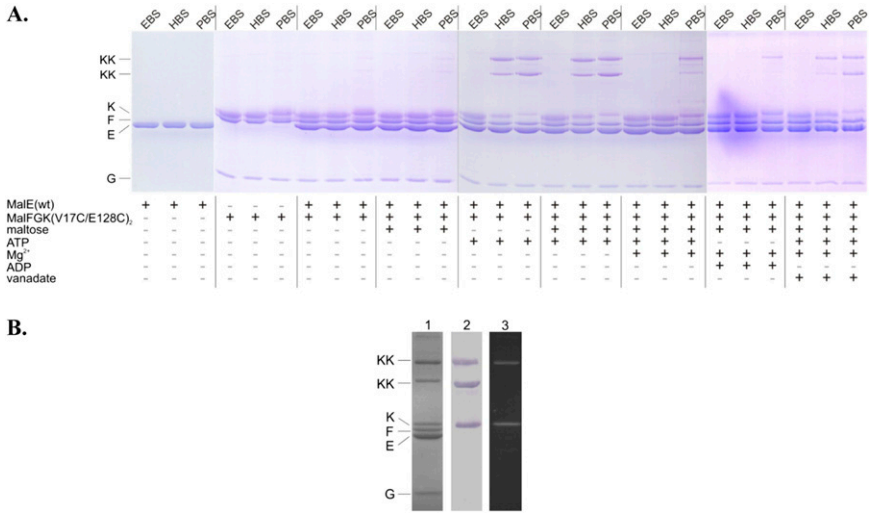

Fig. S6. Site-specific cross-linking of MalFGK(V17C/E128C). (*A*) Purified complex protein was incubated in the absence or presence of wild type MalE with cross-linkers and cofactors as indicated, and subsequently analyzed by SDS/PAGE. (*B*) The cross-linked complex obtained in the presence of wild-type MalE, ATP, and HBS (Coomassie-stained SDS gel, lane 1) was further analyzed by immunoblotting using an antiserum raised against MalK (lane 2), and after additional incubation with MIANS (lane 3) as described in *Materials and Methods*. The MIANS-labeled complex was visualized under UV light following SDS/PAGE. The data reveal that after cross-linking, the upper of the two MalK dimers has still free SH-groups, whereas the lower band cannot be labeled with MIANS. Consequently, we conclude that the lower MalK dimer represents the doubly cross-linked product, whereas the upper band originated from incomplete cross-linking.

Table S1. ATPase activities of maltose transport complex variants

	ATPase activity (μmol P_i min^{-1}·mg^{-1})				
MalE variant	MalF*G*K_2*	MalF*G(T46C)K_2*	MalF*G(P78C)K_2* [MalF*G(P78R1)K_2*]	MalF*G*K(V17C/E128C)$_2$	MalF*G*K(C17R1/C128R1)$_2$
No addition					
In liposomes	0.10 ± 0.02	0.11 ± 0.01	0.07 ± 0.01 [0.05 ± 0.01]	0.11 ± 0.01	0.13 ± 0.01
In detergent solution	0.30 ± 0.03	0.28 ± 0.02	0.23 ± 0.04 [0.25 ± 0.07]	0.37 ± 0.04	0.31 ± 0.02
+ MalE wt					
In liposomes					
– maltose	0.26 ± 0.02	ND	ND	0.19 ± 0.01 (+ DTT)	0.14 ± 0.02
+ maltose	1.60 ± 0.04	1.38 ± 0.10	1.57 ± 0.13 [0.90 ± 0.10]	1.59 ± 0.03 (+ DTT)	1.76 ± 0.06
In detergent solution					
– maltose	0.52 ± 0.03	ND	ND	0.46 ± 0.03 (+ DTT)	0.41 ± 0.05
+ maltose	1.20 ± 0.06	1.00 ± 0.05	0.98 ± 0.07 [0.61 ± 0.05]	1.10 ± 0.04 (+ DTT)	1.07 ± 0.04
+ MalE(G13C)/maltose					
In liposomes	1.71 ± 0.04	ND	1.40 ± 0.13		
In detergent solution	1.26 ± 0.11	ND	0.82 ± 0.08		
+ MalE(T36C)/maltose					
In liposomes	1.34 ± 0.05	ND	1.08 ± 0.09		
In detergent solution	1.09 ± 0.08	ND	0.76 ± 0.03		
+ MalE(T80C)/maltose					
In liposomes	1.55 ± 0.06	ND	1.72 ± 0.04		
In detergent solution	1.14 ± 0.04	ND	1.15 ± 0.09		
+ MalE(S211C)/maltose					
In liposomes	1.55 ± 0.06	1.46 ± 0.04	1.34 ± 0.12		
In detergent solution	1.22 ± 0.16	0.96 ± 0.06	1.06 ± 0.11		
+ MalE(S352C)/maltose					
In liposomes	1.66 ± 0.09	1.30 ± 0.25	1.44 ± 0.11		
In detergent solution	1.25 ± 0.10	0.99 ± 0.14	1.13 ± 0.05		

ATPase activities of purified complex variants in liposomes or detergent solution (0.5 μM) were measured in the absence or presence of de- and renatured MalE variants (5 μM) and maltose (10 μM). Proteoliposomes were prepared as described above. Data generally represent means of at least two independent experiments. ND, not determined; *, cys-less variant; R1, the spin-labeled side chain. For the NBDs' cys-mutants, DTT was added to prevent internal cross-linking of the unlabeled ATPase subunits.

Table S2. Summary of interresidue distances (in Å) determined by site-specific cross-linking in detergent micelles compared with C_α–C_α distances in the available X-ray structures

MalG	MalE	Cα–Cα distance (3PV0) apo	Cα–Cα distance (3PVY) AMP–PNP	Cα–Cα distance (2R6G) ATP	X-link apo-state	X-link + maltose	X-link ATP ± maltose	X-link posthydrolysis	X-link vanadatestate
C78	C13	11	11	10	0–25	0–25	0–25	0–25	0–25
	C36	12	17	18	>5–25	>5–25	>10–25	>5–25	>10–25
	C211	18	25	25	>5–25	>5–25	none (>25)	>5–25	>10–25
	C352	34	42	42	>10–25	>10-25	none (>25)	>10–25	none (>25)
	C246	34	34	33	none (>25)	none (>25)	none (>25)	none (>25)	none (>25)
C46	C211	8	6	6	>5–25	0–25	0–25	0–25	0–25
	C352	21	22	22	0–25	0-25	>10–25	>10–25	>10–25

Underlined distances denote increase in intensity of cross-linked product. MalE-C246 was used as a negative control to demonstrate the reliability of the cross-link approach (Fig. S2). In line with the crystal structures, no cross-link product was obtained.